Graphene oxide reinforced room-temperature-vulcanising elastomers for flexible wave energy converters

Xinyu Wang[1], Maozhou Meng[1], Malcolm Cox[2], Krishnendu Puzhukkil[1], Jingyi Yang[3], Alistair Borthwick[1], Edward Ransley[1], John Chaplin[4], Martyn Hann[1], Robert Rawlinson-Smith[1], Siming Zheng[1], Shanshan Cheng[1], Zhong You[3], Deborah Greaves[1]

Abstract— **Rubber products are widely used for marine applications, such as fenders, bumpers, ship launching airbags, and hovercraft skirts. Many of these products are made through a vulcanising (crosslinking) process where large-scale tooling for high-temperature and high-pressure moulding is required. The cost will be greatly magnified when manufacturing large-scale components, such as flexible parts for next-generation wave energy converters. Two-part polyurethane rubber (PUR) is a room-temperature, low-pressure curing alternative that could minimise manufacturing costs. However, the general inferior mechanical performance of such room-temperature-vulcanising (RTV) rubber (compared to vulcanised rubber) restricts the application of PUR in the marine industry. It has recently been reported that the addition of graphene oxide (GO) could significantly improve the internal bonding of polymer elastomers and thus provide better mechanical performance with a low filler loading. In the work presented in this paper, different types of silane coupling agents (SCA) were used to treat the surface of GO, and the potential application of PUR/GO composites under marine environments and their mechanical performance were investigated. More than 75 % increases in tensile strength were observed after 1 wt % of GO was added. Moreover, a significant reduction in water absorption occurred during the seawater immersion test. It is suggested that hydrophobic sites provided by silane coupling agents play an important role on the GO surface, where polar groups, such as hydroxyl and carboxyl groups, were replaced during the silane treatment.**

Keywords— **Wave energy converters, Flexible materials, Seawater immersion**

Sponsor and financial support acknowledgement: This work was supported in part by the EPSRC grant EP/V040367/1

[1] School of Engineering, Computing and Mathematics, University of Plymouth, Drake Circus, Plymouth PL4 8AA, UK, *xinyu.wang-41@plymouth.ac.uk

[2] Griffon Hoverwork Ltd., Hazel Road, Woolston, Southampton SO19 7GA, UK

[3] Department of Engineering Science, University of Oxford, Parks Road, Oxford, OX1 3PJ, UK

[4] Faculty of Engineering and Physical Sciences, University of Southampton, Southampton SO16 7QF, UK

Digital Object Identifier: https://doi.org/10.36688/ewtec-2023-216

I. INTRODUCTION

A trend favouring incorporating flexible components in wave energy converters is being driven by the lack of survivability in severe conditions, and the poor fatigue performance of the conventional designs comprising entirely rigid components [1, 2]. Flexible components are often manufactured from elastomeric polymer materials and/or their composites. In most existing designs, the flexible parts act as the prime mover by offering a deformable interface between WECs and waves [1]. Some designs utilise elastomer materials as sub-components and benefit from their unique material properties [1, 3]. Dielectric elastomer generators (DEGs) are an emerging technology in the wave energy sectors [4, 5]. In practice, mechanically minimised power take-off (PTO) design can be achieved by either combining DEGs with a primary elastomer mover or simply substituting existing mechanical PTO systems with DEGs. However, research is lacking on material selection, design, and manufacturing process for the elastomer materials that are used in WECs [6].

Natural rubber and different types of synthetic rubbers are the most widely used elastomer materials in products ranging from tiny gaskets to giant ship-launching airbags. These rubber products are usually made through a vulcanising process, where high temperature and high pressure are required [7]. Before vulcanisation, rubber compounds pre-mixed with designated additives in a gum state need to be shaped using moulding or calendaring facilities [8]. Such mouldings are often very expensive because they have to satisfy temperature, pressure, and maintenance requirements. The entire process, including compounding, shaping and vulcanisation, makes rubber manufacturing both "capital- and labour-intensive" [9].

Two-part polyurethane rubber (PUR) is a room-temperature vulcanising (RTV) rubber, that is often used for mould-making and flexible products. This type of rubber is produced by mixing two liquid parts, after which the pourable mixture is cast to solid PUR through a reaction between diisocyanates with polyols [10]. With the aid of catalysts, this reaction can occur at room temperature and atmospheric pressure, reducing the manufacturing cost and potentially having a significant

impact on the Levelized Cost of Energy (LCOE) of flexible WECs. Moreover, the nature of RTV rubber could make the one-piece manufacture of large rubber parts a reality, improving on the present approach of assembling small sub-parts that is widely adopted by rubber product manufacturers for the marine industry. Efforts presently expended on rubber adhesive, moulding, and assembling processes could be largely reduced or even eliminated by applying one-piece manufacturing technology [11].

Graphene oxide (GO) is a two-dimensional monolayer of graphite with oxygen functional groups on the surface. The high aspect ratio and large surface area of GO provide superior interfacial interactions in conventional micro-sized fillers, such as spherical carbon black. This could enable GO to provide a comparable level of tunability regarding the mechanical properties of rubber at lower filler grades, usually below 3 wt.%, compared to the more than 30% grades for conventional micro-fillers [12, 13]. This is very important to PUR casting; in particular, low filler grade leads to a low increase in the viscosity of the mixture and high processability. However, the large interfacial area and the presence of -OH and-COOH groups could potentially cause moisture to be absorbed in the marine environment, and have a negative effect on the mechanical properties of the rubber, e.g. leading to swelling [14].

In this work, a two-part polyurethane rubber (PUR) and graphene oxide are considered with the intention of investigating their potential application in flexible WECs. Two types of silane coupling agents (SCAs) were selected to examine the surface modification of the GO. The SCAs are expected to provide hydrophobic groups on GO and improved interfacial bonding in PUR [15]. A saltwater immersion test was conducted to examine the water absorption capability of PUR/ GO composites. Static uniaxial stretching tests were carried out to evaluate the mechanical performance of the selected PUR and the impact of the GO and SCAs.

II. METHODOLOGY

A. *Materials*

The materials and chemicals used in this work include Xencast® PX30 two-part polyurethane (purchased from

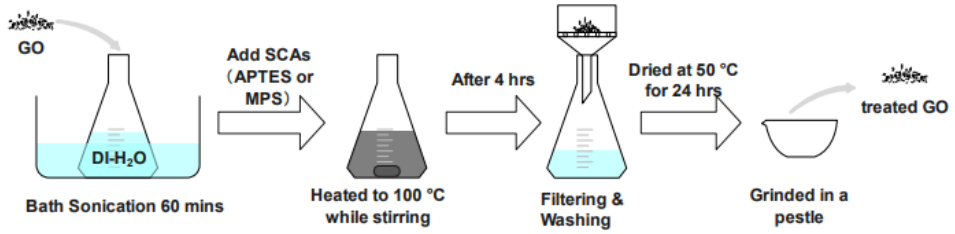

a)

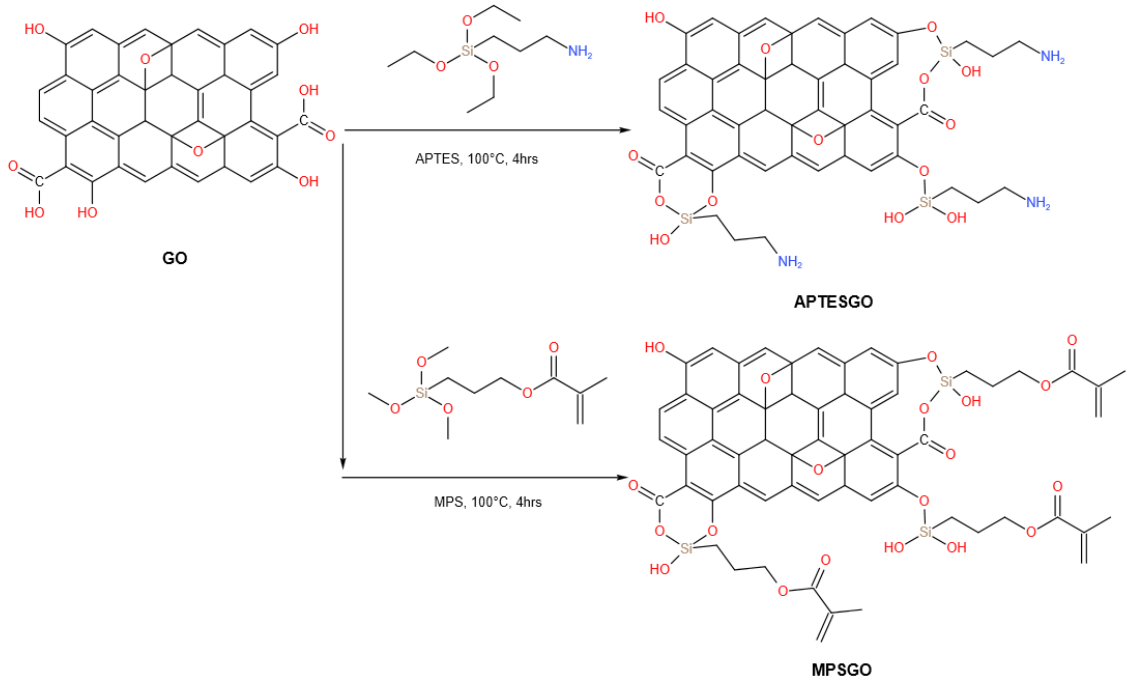

b)

Fig. 1. Illustrations of a) the silane treatment procedure, and b) the grafting mechanism of SCAs on the GO surface

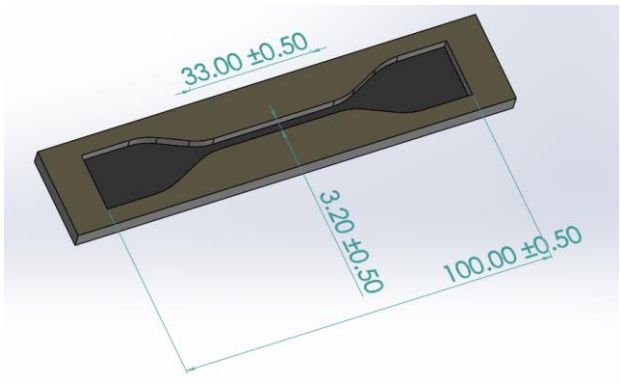

Fig. 2. Dimensions of the mould for tensile tests (unit: mm, samples thickness: 3 mm).

Easy Composites Ltd), Powder-form graphene oxides (supplied by Wholesale Graphene),3-Aminopropyl) triethoxysilane (APTES) and 3-(Methacryloyloxy) propyltrimethoxysilane (MPS) (purchased from Thermo Fisher Scientific).

B. Material preparation

Before the GO was added to PUR, they were treated with APTES and MPS separately, an illustration of SCA treatment is shown in Fig. 1. The silane functionalisation process was as follows, 1) 0.8g of GO was added to 400 ml of DI-water; 2) the mixture was magnetic stirred for 15 min, followed by a bath sonication treatment for 60 min to achieve better dispersion of the GO; 3) 8 ml of silane was added to form the GO+SCA suspension, and then heated to the boiling point of the water and magnetic stirred for 4 hours; 4) the functionalised GO was then filtered and washed with ethanol and DI-water 3 times to remove non-grafted SCAs; and 5) the treated GO was dried at 50 °C for 24 hours and ground into powder form using a pestle.

The GO/PUR composites were prepared by mixing 0.8 g of GO with 40 g of parts B of Xencast® PX30. For better dispersion of treated GO, the mixture was magnetically stirred for 10 min and treated in a sonication bath for 30 mins. Then 40 g of part A was added, and the mixture was stirred vigorously for 1 min. Degassing was performed immediately afterwards at 20 mBar in a vacuum chamber for 1 min to remove air bubbles. The mixture was then poured into 3D-printed PLA moulds (Fig. 2) and cured in the laboratory environment for 24 hrs. The samples were removed from moulds and post-cured for 24 hrs at 55 °C to accelerate the curing process.

C. Experimental set-up

A Bruker ALPHA FT-IR spectrometer was used to examine the SCAs treated GO at Attenuated Total Reflectance (ATR) mode. As-received and treated GO powers were tested from 400 to 4000 wavenumber cm^{-1}.

The JEOL 6610 VP-SEM was used to characterise the as-received GO powders and the fracture surface of the PUR samples after quasi-static uniaxial tensile tests. The samples were coated with gold to prevent charge accumulation on the sample surface.

Saltwater with 3.5 wt% NaCl was used in seawater immersion tests. Samples were dried in an oven at 50°C for 24 hours prior to the immersion. The samples were immersed in salt water at 50 °C for 7 days while the weight of the samples was monitored. The samples were wiped and placed in a lab environment for 10 to 15 mins before weighing to eliminate the error from accumulated water on the surface.

The quasi-static uniaxial tensile tests were carried out on an Instron 3345 universal test machine. The dog-bone-shaped samples following the ASTM D412-06a, die type D, with 3 mm in both width and thickness at the gauge section were adopted (as shown in Fig. 2, 3.2 mm for mould due to the possible shrinkage). The samples were tested at a constant stretching rate of 500 mm/min until rupture happens.

III. RESULTS AND DISCUSSIONS

A. Water absorption

The water uptake of different polyurethane samples was measured by weighing the samples after 1, 2, 3, 4, 5, and 7 days of immersion in salt water at 50 °C. The weight of all samples kept increasing throughout 24 hrs of immersion in water, after which it reached saturation and remained constant, as shown in Fig. 3. PUR filled with 1 wt% of GO exhibited the strongest ability to absorb moisture, with about 1.6 % of additional weight observed. Meanwhile, non-filled PUR and PUR filled with SCA-treated GO behaved similarly, reaching a level of 1.2 to 1.3 % above their original total weights. It should be noted that polyurethane is inherently a hydrophobic polymer, meaning that water could fill interior cavities or those on the surface of the samples [16].

For the GO filler PUR, the water molecules were absorbed by the hydrophilic sites, -COOH and -OH, on the GO surface. In the present work, only 1 wt% of the GO was added and this contributed to ~ 19 % of additional water absorption. After SCA treatment, the

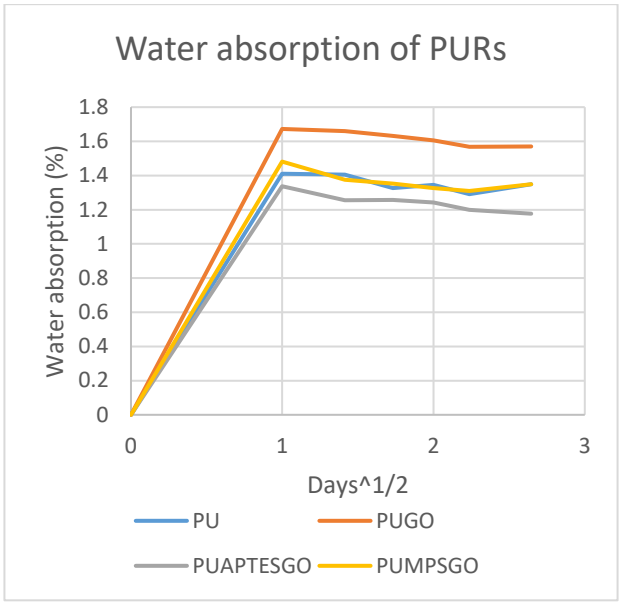

Fig. 3 Water absorption results of different PURs.

hydrophilic sites on hydrophilic sites on GO were replaced by amino (-NH_2) and methacrylate ($CH_2C(CH_3)COO-$) functional groups with reduced water absorption capacity. Therefore, less water was absorbed onto the GO surface when SCA treatment was applied, resulting in a comparable weight gain to that of the non-filled PUR samples. In addition, the organofunctional groups on the surface of the treated GO may provide better compatibility between the GO and the organic PUR matrix, leading to an interfacial region with fewer cavities and imperfections, thus absorbing less water during immersion. The results indicate that the SCA treatment effectively reduced the water absorption of GO-filled PUR, indicating that PUR/GO composites with higher GO loading are potentially feasible in the marine environment.

B. *FTIR spectra results*

Fig. 4 shows the FTIR spectra of as-received GO, APSTE and MPS-treated GO. The data are presented without any offset. The as-received GO samples give an overall lower transmittance than the spectrum of two SCA-treated GO. This is related to the ATR method used and the low reflectance of dark GO. But after SCA surface treatment, the surface reflectance was altered and exhibited a higher overall transmittance level. For As-received GO, the broad peak from 3600 to 2900 cm^{-1} corresponds to hydroxyl groups (-OH) with water molecules absorbed on the GO surface [17]. This feature is significantly reduced in the spectrum of SCA-treated GO, especially for APTESGO, with fewer hydroxyl groups and bonded water molecules appearing on the surface of the SCA-treated GO. The sharp peak at 1706 cm^{-1} for MPSGO is related to the stretching vibration of C=O provided by MPS treatment [18]. A slight shift to a lower wavenumber of this feature can be seen in the spectra for as-received GO, corresponding to the ketone group (C=O) on the GO surface. No peak can be found for APSTEGO in the 1600 to 1710 cm^{-1} wavenumber range. The peak at 1022 cm^{-1} reveals the presence of -COOH on the GO surface for the as-received GO [17]. Sharper peaks on SCA-treated GO at 1004 and 1033 cm^{-1} may be due to the overlapping of Si-O-X and -COOH on the surface of treated GO [19, 20]. Overall, the FTIR results show that the surface chemistry of GO changed significantly after the SCA treatment, proving the effectiveness of the surface treatments.

C. *Uniaxial tensile test results*

Fig. 5 shows the strength and strain curves obtained from uniaxial tensile tests. Although five repeat tests were carried out for each group of samples, only one typical curve closest to the average level is plotted in the Figure. All samples exhibit two near-linear regions in the strength vs strain curves before the fracture.

Fig. 6 shows the average values and the standard deviation of the ultimate tensile strength (UTS, same as the fracture strength here) for different PURs. All GO-filled samples have higher UTS than the non-filled PUR, among which, the PUR filled with APTES-treated GO reaches 1.67 MPa UTS. Compared to the 0.8 MPa for non-filled PUR, an 109 % increase in UTS can be achieved by adding 1 wt% of APTESGO. Due to the non-linearity of the rubber material, the strength at certain strains was used to represent the stiffness of the material, rather than the standard Young's modulus. Here, M100, the "modulus" at 100 % of strain, is shown in Fig. 7. A similar trend can be observed for M100, which is the increment introduced by the addition of GO. APTESGO here shows a better ability in increasing both UTS and M100. W. Xing

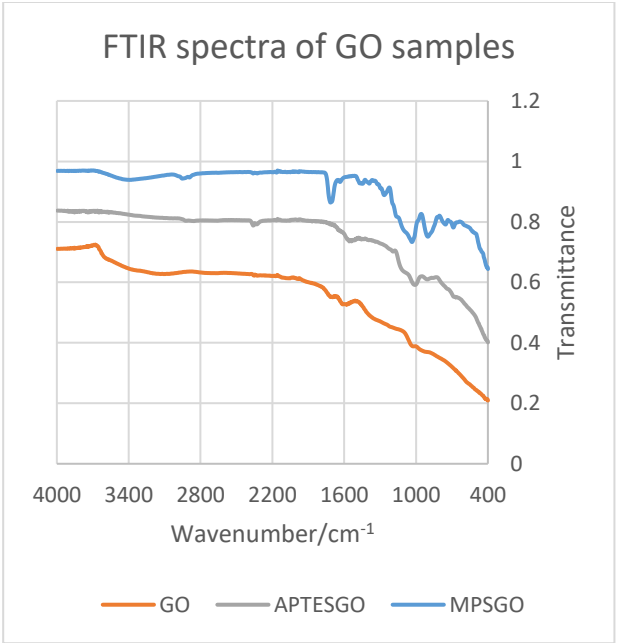

Fig. 4 FTIR spectrum of as-received GO, APTES and MPS treated GO.

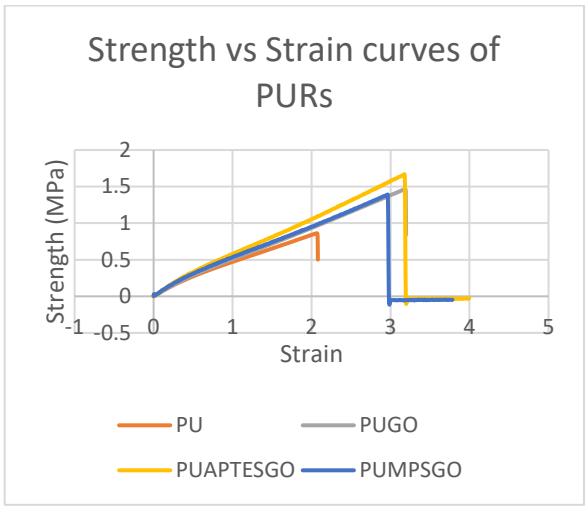

Fig. 5. Strength vs strain curves of different of PURs.

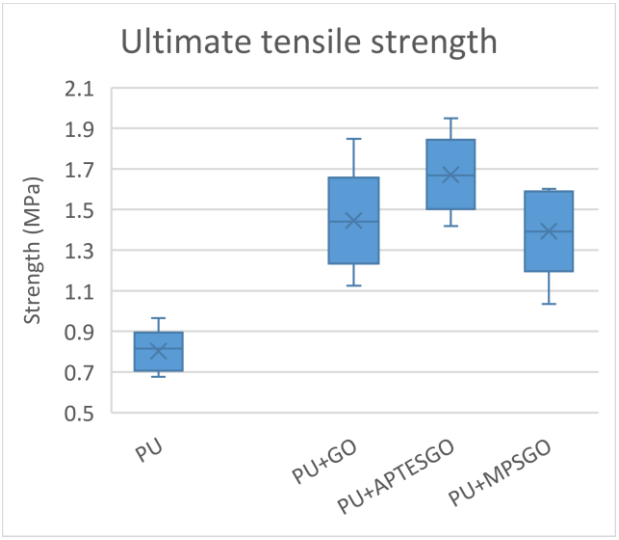

Fig. 6. Ultimate tensile strength of different PURs.

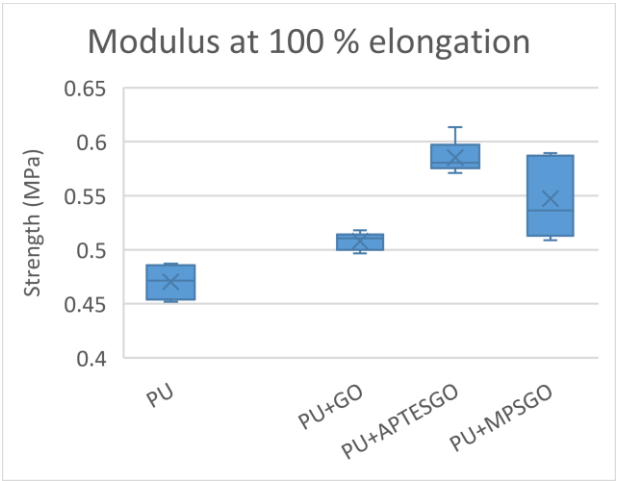

Fig. 7. Modulus of different PURs at 100 % elongation (M100).

et. al. observed a 48 % improvement of UTS by adding 0.5 wt% of graphene in natural rubber and it is suggested graphene with a high specific surface area could provide physical entanglement within rubber chains, resulting in higher fracture strength and modulus [21].

Compared to the graphene fillers, the GO with oxygen content groups can bring additional chemical bindings brought by the reaction between GO and matrix during the curing process, hence further improving the interfacial interaction, which will be discussed later in the SEM results section. The presence of these oxygen content groups could also be reported to act as a linker that creates additional crosslinking networks during the rubber vulcanisation [22]. The strain-induced crystallisation with the addition of GO to natural rubber in elevating the mechanical performance has been widely discussed [12, 23, 24], and M. Tosaka et. al. suggested that this effect is highly dependent on the types of the elastomer matrix [25]. However, there is no evidence that the linker effect and strain-induced crystallisation happen in this work.

S. Woraphutthaporn et. al. applied two different types of SCA with the amino group ending on the GO/natural rubber composites, the results indicate that the SCA treatment could be leading to better GO dispersion and enlarged interfacial regions between GO and rubber. The addition of -NH_2 from SCAs increased the crosslinking density of the rubber during the vulcanisation [19]. A uniform GO dispersion can also be seen in this work when SCA is applied (from the SEM results in Fig. 8), the superior improvement effects provided by APTES to MPS can be related to the different interactions between the PUR matrix and those different functional endings. Further investigations are needed to reveal the chemical interactions caused by GO itself and the addition of SCA with different functional groups, on the PUR matrix and/or the GO to PUR bonding. Ongoing static and fatigue testing of seawater-immersed samples are expected to provide a broader understanding of PUR/GO composites for future applications of flexible wave energy converters, where rubber components are designed to withstand years of cyclic loading in the marine environment.

D. SEM results

The SEM results of as-received GO are shown in Fig. 8a, in which the agglomerations of GO plates are identified, giving aggregates from 1 to 10 μm in size. The GO sheets with large surface areas tend to stack together to form agglomerations. Identical morphology was also observed in [26]. Fig. 8b to 8f reveal the fracture surface of different PUR samples after the uniaxial tensile test. The non-filled PUR shown in Fig. 8b has a flat and smooth fracture surface, however, no obvious microstructure can be observed. The fracture surface of GO-filled PUR is having a significantly higher surface roughness and convex edges derived from GO fillers can be seen, especially for APTESGO-filled PUR. Linear edges originating from the presence of GO particles or

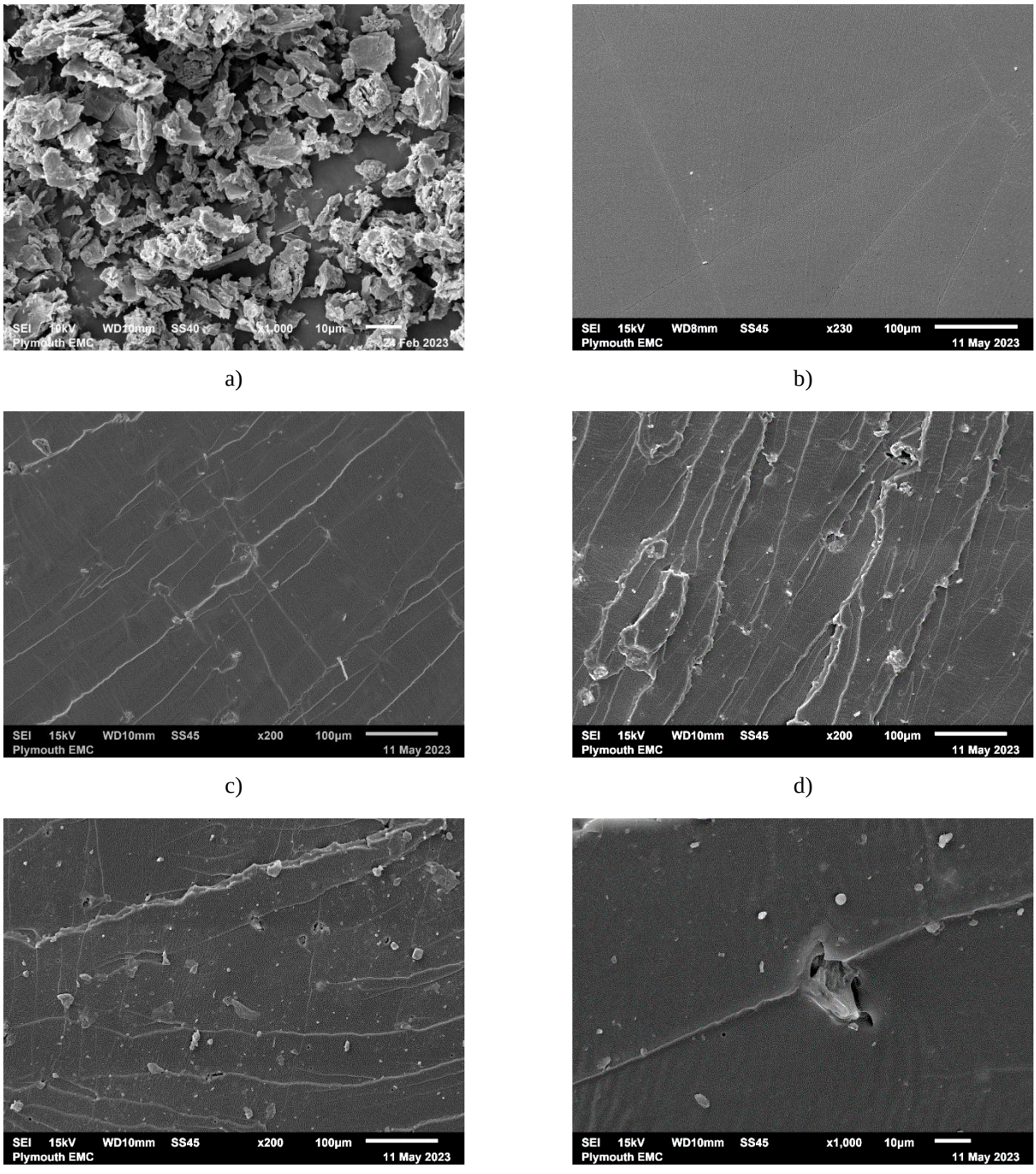

Fig. 8. SEM image of a) as-received GO, and the fracture surface of b) PU, c) PU+GO, d) PU+APTESGO, e & f) PU+MPSGO

aggregates were interrupted when encountering other GO particles or aggregates, then continued or branched from the interruption point. The dispersion states are hard to observe directly due to the surface roughness of the filled samples. However, the higher density of the convex structures in PUR with SCA-treated GO reflects the fact that a better dispersion of GO can be achieved by SCA treatment, especially with APTES.

Fig. 8f shows cavities adjacent to the GO aggregates when MPS is applied, while fewer features could be found when APTES is added. This could be related to the better compatibility of APTES-treated GO with PUR than that of the MPS treatment. Referring to the improved UTS discussed in the previous section, it is suggested that the presence of GO particles is preventing the breaking of PUR and provides a bridging effect [26, 27]. The APTES-treated GO leads to a better bonding effect by increased interfacial adhesion and the larger interfacial area results from an improved dispersion state of the GO fillers [28]. Meanwhile, the weaker improvement in GO dispersion and more imperfections observed in PUR filled with MPSGO matches its little effects on the mechanical properties of the GO/PUR composites.

IV. CONCLUSION

In this study, the effects of GO and SCA treatment on the tensile properties and water absorption ability of an RTV polyurethane rubber was investigated. Two different types of SCA were applied and APTES shows the best performance to improve the tensile strength by providing a better GO dispersion and an increased interfacial bonding between GO and PUR matrix. 109 % of the UTS and 48 % of modulus at 100 % of strain were achieved by adding 1 wt% of APTES treated GO. The SCA coating is also providing a hydrophobic shell to repel the water molecule to the surface of GO filler, which suggests the SCA-treated GO/PUR composites have a great potential for future flexible wave energy convertors with rubber components.

ACKNOWLEDGEMENT

This work was supported by the Engineering and Physical Sciences Research Council (EPSRC) [Grant number EP/V040367/1].

REFERENCES

[1] I. Collins, M. Hossain, W. Dettmer, and I. Masters, "Flexible membrane structures for wave energy harvesting: A review of the developments, materials and computational modelling approaches," *Renewable and Sustainable Energy Reviews,* vol. 151, p. 111478, 2021.

[2] K. Di *et al.*, "Dielectric elastomer generator for electromechanical energy conversion: A mini review," *Sustainability,* vol. 13, no. 17, p. 9881, 2021.

[3] Q. Ltd., "AISV - Automatically Inflatable and Stowable Volume," Wave Energy Scotland, 2016.

[4] T. Andritsch *et al.*, "Challenges of using electroactive polymers in large scale wave energy converters," in *2012 Annual Report Conference on Electrical Insulation and Dielectric Phenomena*, 2012: IEEE, pp. 786-789.

[5] R. Vertechy and M. Fontana, "Dielectric elastomers for wave energy harvesting," *SPIE Newsroom,* pp. 148-156, 2015.

[6] D. Aravind *et al.*, "Feasibility of elastomeric composites as alternative materials for marine applications: A compendious review on their properties and opportunities," *Proceedings of the Institution of Mechanical Engineers, Part M: Journal of Engineering for the Maritime Environment,* p. 14750902221095321, 2022.

[7] N. Mandlekar, M. Joshi, and B. S. Butola, "A review on specialty elastomers based potential inflatable structures and applications," *Advanced Industrial and Engineering Polymer Research,* 2021.

[8] B. Rodgers, *Rubber compounding: chemistry and applications*. CRC press, 2015.

[9] J. G. Sommer, *Engineered rubber products*. Hanser, 2009.

[10] K. Hanhi, M. Poikelispaa, and H. M. Tirila, "Elastomeric materials," *Tampere University of Technology, Tampere,* 2007.

[11] N. S. Cheekuramelli, D. Late, S. Kiran, and B. Garnaik, "Engineering applications of elastomer blends and composites," in *Elastomer Blends and Composites*: Elsevier, 2022, pp. 57-81.

[12] L. Zhao, X. Sun, Q. Liu, J. Zhao, and W. Xing, "Natural rubber/graphene oxide nanocomposites prepared by latex mixing," *Journal of Macromolecular Science, Part B,* vol. 54, no. 5, pp. 581-592, 2015.

[13] S. C. Bhatia and A. Goel, *Rubber Technology: Two Volume Set* (no. v. 1-2). Woodhead Publishing India PVT. Limited, 2019.

[14] B. Lian *et al.*, "Extraordinary water adsorption characteristics of graphene oxide," *Chemical science,* vol. 9, no. 22, pp. 5106-5111, 2018.

[15] T. Nakamura, H. Tabuchi, T. Hirai, S. Fujii, and Y. Nakamura, "Effects of silane coupling agent hydrophobicity and loading method on water absorption and mechanical strength of silica particle‐filled epoxy resin," *Journal of Applied Polymer Science,* vol. 137, no. 17, p. 48615, 2020.

[16] T. J. Benjamin, L. J. Yu, D. A. Thomas Raymond, and N. Y. G. Lai, "Preparation and Water Absorption Analysis of Polyurethane Foam Reinforced Sawdust Composites," in *Enabling Industry 4.0 through Advances in Manufacturing and Materials: Selected Articles from iM3F 2021, Malaysia*: Springer, 2022, pp. 317-326.

[17] G. Surekha, K. V. Krishnaiah, N. Ravi, and R. P. Suvarna, "FTIR, Raman and XRD analysis of graphene oxide films prepared by modified Hummers method," in *Journal of Physics: Conference Series*, 2020, vol. 1495, no. 1: IOP Publishing, p. 012012.

[18] I. Chung *et al.*, "Preparation, stabilization and characterization of 3-(methacryloyloxy) propyl trimethoxy silane modified colloidal nanosilica particles," *Colloids and Surfaces A: Physicochemical and Engineering Aspects,* vol. 585, p. 124066, 2020.

[19] S. Woraphutthaporn, P. Pattananuwat, C. Hayichelaeh, T. Kobayashi, and K. Boonkerd, "Enhancing the properties of graphene oxide/natural rubber nanocomposite‐based strain sensor modified by amino‐functionalized silanes," *Polymers for Advanced Technologies,* vol. 33, no. 10, pp. 3386-3398, 2022.

[20] J. J. Senkevich, C. J. Mitchell, G.-R. Yang, and T.-M. Lu, "Surface chemistry of mercaptan and growth of pyridine short-chain alkoxy silane molecular layers," *Langmuir,* vol. 18, no. 5, pp. 1587-1594, 2002.

[21] W. Xing, J. Wu, G. Huang, H. Li, M. Tang, and X. Fu, "Enhanced mechanical properties of graphene/natural rubber nanocomposites at low content," *Polymer international,* vol. 63, no. 9, pp. 1674-1681, 2014.

[22] B. Mensah, D. S. Konadu, and B. Agyei-Tuffour, "Effects of graphene oxide and reduced graphene oxide on the mechanical and dielectric properties of acrylonitrile-butadiene rubber and ethylene-propylene-diene-monomer blend," *International Journal of Polymer Science,* vol. 2022, 2022.

[23] B. Ozbas *et al.*, "Strain‐induced crystallization and mechanical properties of functionalized graphene sheet‐filled natural rubber," *Journal of polymer science part B: Polymer physics,* vol. 50, no. 10, pp. 718-723, 2012.

[24] X. Wu, T. Lin, Z. Tang, B. Guo, and G. Huang, "Natural rubber/graphene oxide composites: Effect of sheet size on mechanical properties and strain-induced crystallization behavior," *Express Polymer Letters,* vol. 9, no. 8, 2015.

[25] M. Tosaka *et al.*, "Crystallization and stress relaxation in highly stretched samples of natural rubber and its synthetic analogue," *Macromolecules,* vol. 39, no. 15, pp. 5100-5105, 2006.

[26] J. Wilk, R. Smusz, R. Filip, G. Chmiel, and T. Bednarczyk, "Experimental investigations on graphene oxide/rubber composite thermal conductivity," *Scientific reports,* vol. 10, no. 1, p. 15533, 2020.

[27] J. H. Lee and S. H. Kim, "Fabrication of silane-grafted graphene oxide and its effect on the structural, thermal, mechanical, and hysteretic behavior of polyurethane," *Scientific reports,* vol. 10, no. 1, p. 19152, 2020.

[28] Y. Zhang *et al.*, "Silane-Modified graphene oxide composite as a promising corrosion-inhibiting film for magnesium alloy AZ31," *Frontiers in Materials,* vol. 8, p. 737792, 2021.